Mon. Not. R. astr. Soc. (1986) **220,** 513–528

MERLIN observations of the circumstellar envelope of VX Sagittarius

Jessica M. Chapman and R. J. Cohen *University of Manchester, Nuffield Radio Astronomy Laboratories, Jodrell Bank, Macclesfield, Cheshire SK11 9DL*

Accepted 1985 December 31. Received 1985 December 31; in original form 1985 October 3

Summary. MERLIN maps of the H_2O and OH maser emission from the circumstellar envelope of the supergiant star VX Sagittarius are presented. The OH masers at 1612 MHz are at a radial distance of 2×10^{16} cm from the star and lie in a 'thin-shell' region which has an expansion velocity of $\sim$19 km s^{-1}. The H_2O masers occur nearer the star in an accelerating 'thick-shell' region which has a mean radius of $\sim3\times10^{15}$ cm and a mean expansion velocity of $\sim$9 km s^{-1}. The OH mainline masers have angular and velocity extents similar to those of the H_2O masers and are believed to lie in the same thick shell, although absolute position measurements are needed to confirm this. The distribution of masers in this inner region is asymmetric. This may be due to the influence of the stellar magnetic field. The magnetic field in the envelope is determined from Zeeman splitting of the OH mainlines to be $\sim$2 mG. The velocity field of the circumstellar envelope as traced by SiO, H_2O and OH maser lines cannot be driven by a $1/R^2$ radiation pressure law with constant dust opacity. It is suggested that the driving force per unit mass increases outwards to a distance of at least 50 stellar radii.

1 Introduction

Radio maser emission from OH, H_2O and SiO molecules provides a means of studying the circumstellar envelopes of long-period variable stars. Each maser line requires different conditions for its excitation and probes a different region of the circumstellar envelope. The OH 1612-MHz maser emission arises in the cool outer parts of the envelopes at distances of $\sim10^{16}$ cm or more from the central star. Aperture synthesis radio maps of the 1612-MHz emission of some 30 sources made with MERLIN and the VLA have shown clear evidence for expanding envelopes, with mass-loss rates of typically $10^{-5}\,M_\odot\,\mathrm{yr}^{-1}$ (Booth *et al.* 1981; Bowers, Johnston & Spencer 1981; Diamond *et al.* 1985 and references therein). The 1612-MHz masers are pumped by far-infrared photons and the details of the pumping mechanism for this line are well established (Elitzur 1982).

Other maser lines from OH at 1665/1667 MHz, H_2O at 22 GHz and SiO at 43/86 GHz are potentially valuable probes of the warmer inner regions of the envelope. Far fewer sources have been mapped in these lines and their pumping mechanisms are less well understood. The

envelope dynamics and the structure of the inner regions are also not well understood. Part of the difficulty has been the lack of good interferometer data. There is a need to obtain comprehensive observations of a few well-chosen sources. In this paper we present MERLIN observations of the OH and H_2O masers in the circumstellar envelope of the luminous supergiant star VX Sagittarius (hereafter VX Sgr). The new results are combined with published measurements of the SiO masers (Lane 1984) to give the most comprehensive radio picture of an oxygen-rich circumstellar envelope available to date.

VX Sgr is a semi-regular variable with an optical period of 732 day (Kukarkin *et al.* 1970) and a spectral classification which varies between M4e–Ia and M9.5. From its galactic coordinates it is a possible member of the Sgr OB1 association in the Carina spiral arm which is at an estimated distance of 1.7 kpc (Humphreys, Strecker & Ney 1972). For this distance the stellar luminosity determined from the IR flux densities of Humphreys (1974) is $L_*{\sim}4.2{\times}10^5\,L_\odot$ and the stellar radius for a photospheric temperature of 2500 K is $R_*{\sim}2.4{\times}10^{14}$ cm. For this luminosity the stellar mass M_* is expected to be at least $10\,M_\odot$ (Paczyński 1970).

VX Sgr is one of the most luminous stars known and has an extremely high mass-loss rate which is estimated from the infrared luminosity and envelope expansion velocity to be approximately $2.5{\times}10^{-4}\,M_\odot\,\mathrm{yr}^{-1}$ (Engels *et al.* 1983). The circumstellar envelope is a strong source of maser emission. OH, H_2O and SiO spectra are presented in Fig. 1 together with a schematic summary of the interferometer data showing the locations of the different emitting regions.

In Section 2 we describe the MERLIN observations and data analysis. In Section 3 we give the results and in Section 4 we discuss the spatial, velocity and magnetic field structure of the circumstellar envelope of VX Sgr.

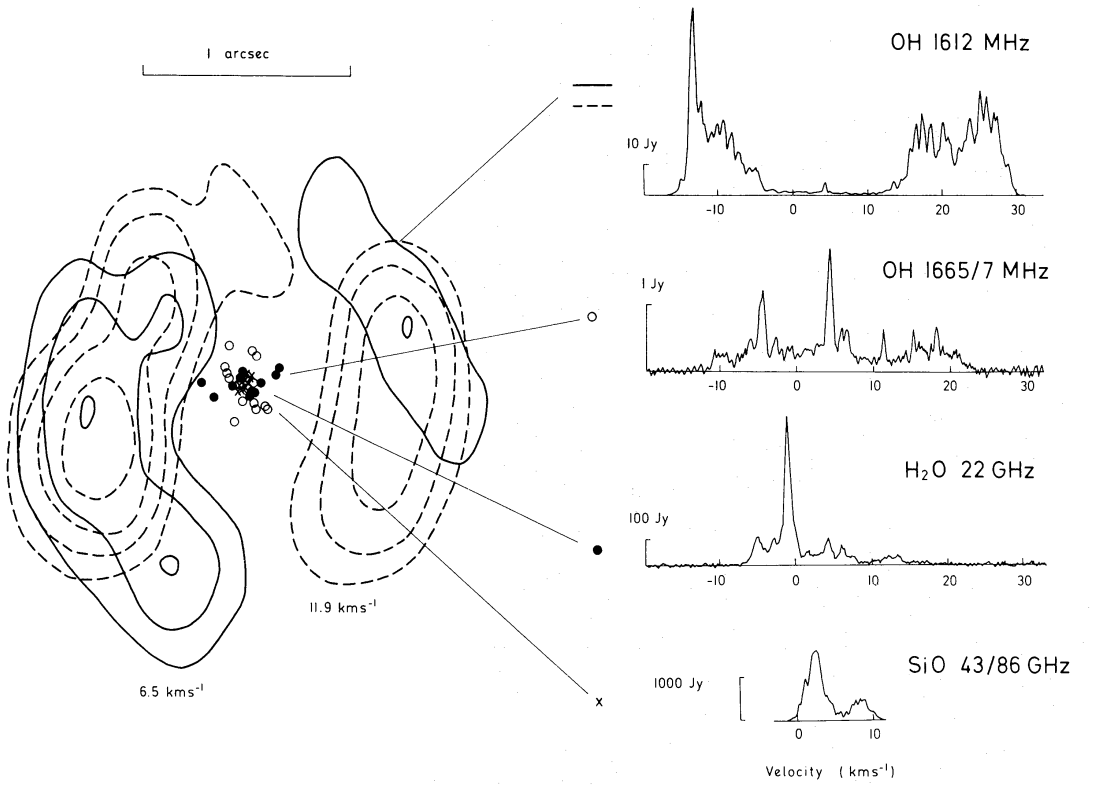

Figure 1. Total power spectra of the maser emission from VX Sgr together with a schematic summary of the interferometer data showing the locations of the different masing regions. Note that the OH emission at 1612 MHz is only shown for two line-of-sight velocities, 6.5 km s^{-1} (solid contours) and 11.9 km s^{-1} (dashed contours). The stellar velocity is ~5.5 km s^{-1}. The SiO results are from Lane (1984).

2 Observations and data analysis

The observations of the OH masers were taken in 1983 January using four telescopes of the MERLIN network. These were the MKIA telescope at Jodrell Bank and outstation telescopes at Wardle, Knockin and Defford. The longest baseline (MKIA – Defford) is 127 km which corresponds to a lobe spacing of ~0.3 arcsec at the OH line frequencies. Observations were taken at the satellite-line frequency of 1612 MHz in left-hand circular (LHC) polarization and at the mainline frequencies of 1665 and 1667 MHz in right-hand circular (RHC) polarization. On each occasion VX Sgr was tracked for 6.5 hr.

During the observations the cross-correlation functions for each baseline were obtained on-line using 160 channels of a digital correlator. They were weighted off-line with a triangular weighting function and Fourier transformed to give 80-channel cross-correlation spectra for each integration. The instrumental phase and amplitude variations across the spectral bandpasses were calibrated using observations of the unresolved continuum source 2134+004, the flux density of which was taken to be 4.2 Jy. A spectral bandwidth of 312.5 kHz was used, giving a total velocity range of 56 km s^{-1} for the mainlines and 58 km s^{-1} for the 1612-MHz line. In each case the velocity resolution was 1.1 km s^{-1}. For the 1612-MHz data the channel with the strongest emission was mapped first using the standard closure-phase technique of Cornwell & Wilkinson (1981). This channel was then used as a phase reference for the other frequency channels which, after phase-referencing, were mapped by Fourier-inverting the data and then using the CLEAN procedure (Högbom 1974). The relative positions of the emission features at 1612 MHz were measured from the channel maps to a precision of ~0.06 arcsec. Maps were also obtained of the emission averaged over several adjacent channels.

The OH mainline emission from VX Sgr at 1665 and 1667 MHz is much weaker than the 1612-MHz emission (see Fig. 1). At 1665 and 1667 MHz it was only possible to use the data on the three MKIA baselines and therefore no closure phases were available. Nevertheless, at our angular resolution the mainline masers are unresolved point sources. The brightest feature at each line was used as a phase reference to correct the phases in the other frequency channels before mapping. The relative positions of the masers were obtained by fitting two-dimensional Gaussian components to the point sources in each channel map. The positions of the 1665-MHz masers relative to the 1667-MHz masers were not measured directly.

The H_2O masers were observed in LHC polarization in 1983 March for 5.5 hr. Three outstation telescopes at Tabley, Darnhall and Knockin were used. The longest baseline was 67 km which at the frequency of 22 GHz gives a lobe spacing of 0.04 arcsec. For these observations the spectral bandwidth was 2.5 MHz, the total velocity range was 34 km s^{-1} and the velocity resolution of each channel was 0.8 km s^{-1}. The strongest feature was an unresolved point source which was taken as both an amplitude and phase reference for the data in the other channels. We did not have an absolute flux calibration for these MERLIN 22-GHz observations and so the flux densities of the H_2O masers were obtained relative to that of the reference feature. Each frequency channel showed one or more point sources and the relative positions were found by fitting Gaussian components to the features in the channel maps.

3 Results

3.1 THE OH 1612-MHz MASERS

The 1612-MHz single-dish spectrum and the MERLIN maps obtained by averaging the data over several frequency channels are shown in Fig. 2. The velocity range of each of the maps is indicated on the spectrum and the mid-velocity is given in the top left-hand corner of the corresponding map. The maps are in good agreement with the expanding-shell model by Reid *et al.* (1977) in

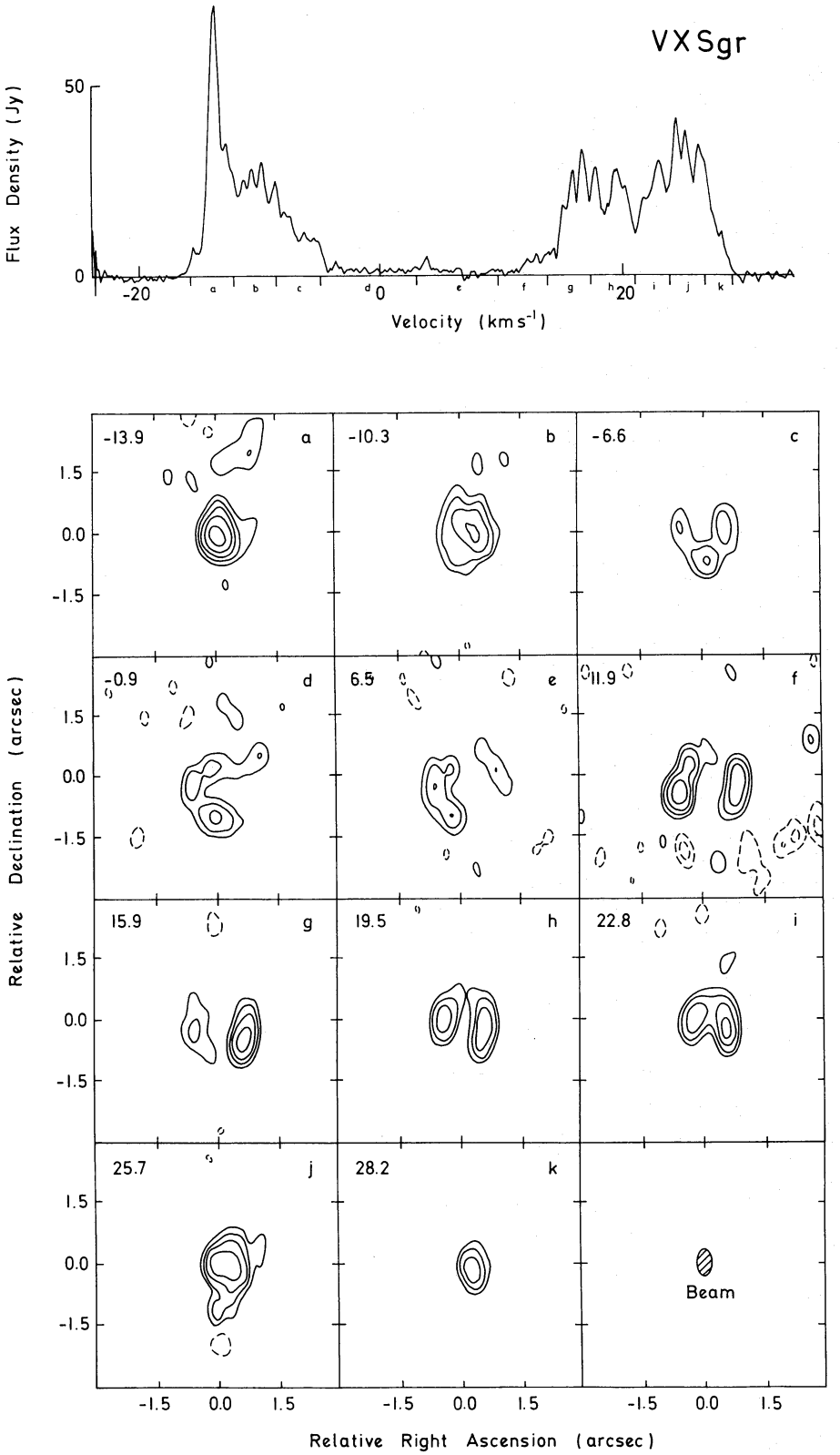

Figure 2. Single-dish spectrum of VX Sgr obtained in 1982 October with a velocity resolution of 0.2 km s^{-1}. The maps were obtained from MERLIN observations in 1983 January. The central velocities are marked in the upper left-hand corners and the letters correspond to the velocity intervals marked on the spectrum. Map a was used as the reference. For maps a–c and g–k the contour levels are at 0.6, 1.2, 2.4, 4.8 and 9.6 Jy/beam area. For maps d–f the contour levels are at 0.05, 0.1, 0.2 and 0.4 Jy/beam area. Negative contours are shown by dashed lines. The elliptical restoring beam is also shown.

which the maser emission originates in the outer parts of the envelope where the gas is moving at or close to terminal velocity. The stellar velocity is approximately at the centre of the 1612-MHz profile and the velocity separation of the extreme blue and redshifted emission features is approximately twice the envelope expansion velocity at the radius of the 1612-MHz masers. The emission at the extreme blue and redshifted velocities (maps a and k) comes from cap-like regions at the front and back of the star which are close to the line-of-sight through the stellar position. At the intermediate velocities, segments of shell-like structures are observed. For maps d–h the strongest emission occurs to the east and west, with weak or no emission in the north and south, indicating that either the distribution of OH or the maser excitation is not uniform in the circumstellar envelope.

For an envelope expanding with a velocity V_E at the radius R, emission at the line-of-sight velocity $V-V_*$ relative to the stellar velocity V_* will arise from a ring or ring segment whose projected separation A from the stellar position satisfies

$$\frac{(V-V_*)^2}{V_E^2}+\frac{A^2}{R^2}=1 \qquad (1)$$

(Reid *et al.* 1977). We have used a least-squares minimization programme to determine the best-fitting values of the stellar position relative to the map centres, the stellar velocity, the expansion velocity V_E and the angular radius of the shell R_A. For the 1612-MHz masers these are

$V_*=5.3\pm0.4\,\mathrm{km\,s^{-1}}$

$V_E=18.6\pm0.9\,\mathrm{km\,s^{-1}}$

$R_A=0.83\pm0.05$ arcsec

right ascension offset $=-0.12$ arcsec

declination offset $=-0.14$ arcsec.

The angular radius of 0.83 arcsec corresponds to a linear radius of $R=2.1\times10^{16}$ cm at the assumed distance of 1.7 kpc.

3.2 THE OH MAINLINE AND H_2O MASERS

Maps were made of the OH 1665/7 MHz emission at velocities between -5 and 15 $\mathrm{km\,s^{-1}}$. Six unresolved features were detected at 1665 MHz, and eight unresolved features were detected at

Table 1. Relative positions of the OH masers in VX Sgr, 1665-MHz RHC (1983 February).

Velocity $\mathrm{km\,s^{-1}}$	n	R.A. Offset (arcsec)	Dec Offset (arcsec)	Peak Flux Density (Jy)
14.8	3	0.08+	0.05	0.2
6.2	1	0.00	0.21	0.2
3.7	4	0.11	0.16	0.8
0.4	4	0.07	0.10	0.3
-1.8	2	-0.01+	-0.02	0.3
-4.7#	2	0.00	0.00	1.4

phase reference

+ positional errors ± 0.04 arcsec

Table 2. Relative positions of the OH masers in VX Sgr, 1667-MHz RHC (1983 February).

Velocity	n	R.A. Offset	Dec Offset	Peak Flux Density
km s^{-1}		(arcsec)	(arcsec)	(Jy)
15.6	2	0.08	0.08	0.5
6.3	1	-0.01	0.20	0.2
5.1	2	0.08	0.08	1.2
3.4	1	0.11	0.12	0.4
3.4	2	0.10	0.24	0.2
-0.6	4	-0.05	0.02	0.3
-3.2	2	0.01	0.04	0.4
-4.5#	2	0.00	0.00	2.0

phase reference

1667 MHz. Each feature was observed at the same relative position in one to four adjacent maps. The relative positions of the features, their peak flux densities, the weighted mean velocities and the number n of channels which have been averaged are given in Tables 1 and 2. The positions of the 1665-MHz masers relative to the 1667-MHz masers were not measured directly but can be estimated with confidence because of strong similarities in the two sets of maps. The maps were

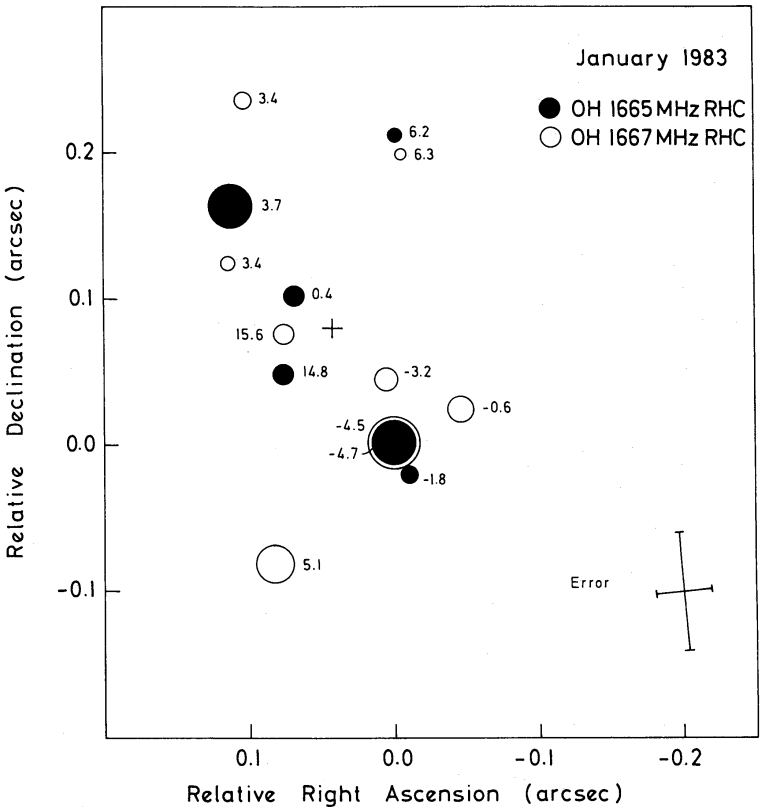

Figure 3. The relative positions of the RHC polarized OH mainline masers of VX Sgr. The areas of the circles are proportional to the total fluxes of the features. The position of the 1665-MHz masers were not measured with respect to the positions of the 1667-MHz masers, but we are able to align the relative positions at the two frequencies as the -4.5-km s^{-1} feature at 1667 MHz and the -4.7-km s^{-1} feature at 1665 MHz belong to a Zeeman quartet (Section 4.4). The cross shows the centroid of emission at each frequency.

aligned assuming that the 1665-MHz feature at $-4.7\,\mathrm{km\,s^{-1}}$ and the 1667-MHz feature at $-4.5\,\mathrm{km\,s^{-1}}$ coincide. Evidence is presented in Section 4.4 below that these features are part of a Zeeman group. Once this alignment is adopted it is then found that three further 1665-MHz features with velocities of 3.7, 6.2 and $14.8\,\mathrm{km\,s^{-1}}$ coincide within the measurement errors with 1667-MHz features at similar velocities of 3.4, 6.3 and $15.6\,\mathrm{km\,s^{-1}}$ respectively. The centroids of emission at the two frequencies also coincide. The relative positions of all the OH mainline masers, aligned in this way, are plotted in Fig. 3. The mainline masers occupy a region of angular extent ~0.3 arcsec in the north–south direction and ~0.15 arcsec in the east–west direction.

The maps of the H_2O maser emission show 15 unresolved masers. The relative positions and fluxes of these are given in Table 3 and are plotted in Fig. 4. The maximum angular extent of the H_2O emission region is ~0.3 arcsec in the east-west direction and ~0.1 arcsec in the north–south direction. The H_2O and OH mainline masers thus occupy regions of similar maximum angular extent ~0.3 arcsec, corresponding to a linear extent of $\sim 8\times10^{15}$ cm, although the two distributions are elongated in approximately orthogonal directions. The H_2O and OH mainline masers also have similar velocity extents. Their velocity fields seem chaotic in comparison with the highly ordered thin-shell velocity pattern of the OH 1612-MHz masers and may be more turbulent. There is evidence for large-scale regularity, however, as we now discuss.

4 Discussion

4.1 STRUCTURE OF THE CIRCUMSTELLAR ENVELOPE

The MERLIN maps of the OH and H_2O masers of VX Sgr and the VLBI maps of the SiO masers by Lane (1984) together probe a wide range of locations in the circumstellar envelope, from

Table 3. Relative positions of the H_2O masers in VX Sgr, 2.2 GHz (1983 March).

Velocity	n	R.A. Offset (arcsec)	Dec Offset (arcsec)	Relative Peak flux Density (%)
-5.6	5	0.03	-0.03	10
-5.0	5	0.12	-0.02	13
-4.3	4	0.04	-0.04	10
-2.7	7	-0.04	-0.04	18
-2.0	3	-0.08	0.04	6
-1.8	3	0.04+	-0.06+	16
-0.9#	6	0.00	0.00	100
0.1	3	-0.01++	0.00++	18
1.9	3	0.09	0.02	5
3.0	4	0.19	-0.08	4
3.4	2	0.09	0.02	5
4.6	5	0.18	-0.05	20
6.3	4	0.07	0.04	9
7.8	3	0.06	0.04	3
12.3	2	-0.13	-0.02	5

\# phase and amplitude reference
\+ positional errors ± 0.05 arcsec
++ positional errors ± 0.07 arcsec

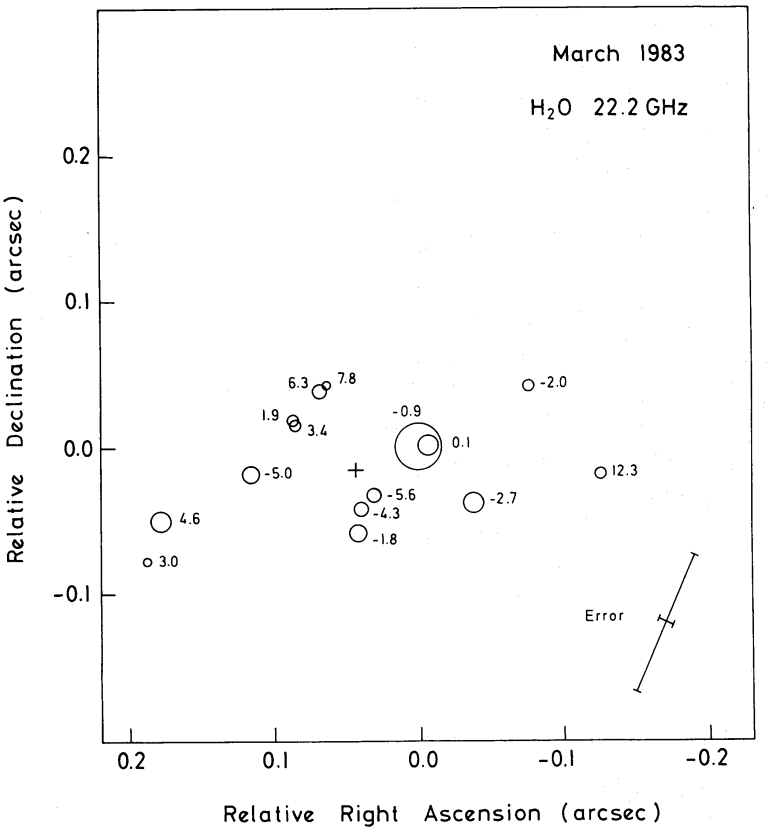

Figure 4. The relative positions of the H_2O masers of VX Sgr. The areas of the circles are proportional to the total fluxes of the features. The cross shows the centroid of the emission.

positions only $\sim 3\times10^{14}$ cm above the photosphere to the cool outer regions at distances of $\sim 2\times10^{16}$ cm from the star. In order to make full use of the available kinematic information, the sets of maps of the OH 1612-MHz, OH 1665/7-MHz, H_2O and SiO masers need to be aligned. As the absolute positions of the masers have not been measured, some assumptions are needed to align the maps. VLA and MERLIN measurements suggest that in general the emission centroids of circumstellar OH and H_2O masers coincide with the stellar position to within ~ 0.1 arcsec (Johnston, Spencer & Bowers 1985; Diamond *et al.* 1985; Chapman & Cohen 1985). For VX Sgr we assume that

(i) The centroids of the SiO, H_2O and OH mainline maser emission coincide with the stellar position. Centroids are marked in Figs 3 and 4 by crosses.

(ii) The stellar position is the expansion centre determined by fitting to the OH 1612-MHz data (Section 3.1).

It will be important to check these assumptions by accurate astrometry. Meanwhile we adopt them as reasonable working hypotheses. The various data sets can then be aligned as shown in Fig. 1, and the combined data can be used to investigate the envelope structure and kinematics.

We note first that the maser regions form a natural sequence of layers about the star as expected from consideration of line-excitation requirements (Olnon 1977; Elitzur 1981). The high-excitation SiO masers occur closest to the star. The SiO lines are rotational transitions of vibrationally excited states some ~ 2000 K above their ground state. Collisional pumping is likely for these masers, with high densities up to $\sim 10^{12}$ cm^{-3} (Elitzur 1980). The H_2O 22-GHz maser line is also a high-excitation transition between the 6_{16} and 5_{23} rotational levels each ~ 650 K

above the ground state. It is therefore natural to find the H_2O masers in a layer around the SiO masers. Collisional pumping is also suggested for the H_2O masers, with densities of up to $\sim 10^{10}\,cm^{-3}$ (Cooke & Elitzur 1985). The OH mainlines are ground-state hyperfine lines, but maser inversion requires the OH to cycle through excited rotational states some 100–400 K above the ground state. Pumping schemes for these masers require them to occur in warm optically thin parts of the circumstellar envelope, at densities of up to $\sim 10^{7}\,cm^{-3}$ (Elitzur 1978). For a spherically symmetric outflow the theoretical models therefore predict that the OH mainline masers occur at greater radii than the H_2O masers. For VX Sgr a surprising result is that the OH mainline masers appear to be coextensive with the H_2O masers. If the OH and H_2O masers are at similar radial distances as suggested by their similar angular and velocity extents, then some density asymmetry in the inner circumstellar envelope is indicated. Some asymmetry is also suggested by the orthogonal elongated distributions of the H_2O and OH mainline masers (Section 4.3). Finally, as expected, the OH 1612-MHz masers occur in the cool, optically thick outer layers of the envelope (Elitzur, Goldreich & Scoville 1976).

We now consider the envelope kinematics. In Fig. 5 the velocities of the SiO, H_2O and OH masers of VX Sgr are plotted against their projected spatial off-sets from the adopted stellar position. The stellar velocity was taken to be $V_* = 5.3\,km\,s^{-1}$ as determined from the fit to the OH 1612-MHZ data (Section 3.1). The thin-shell model fitted to the OH 1612-MHZ data is

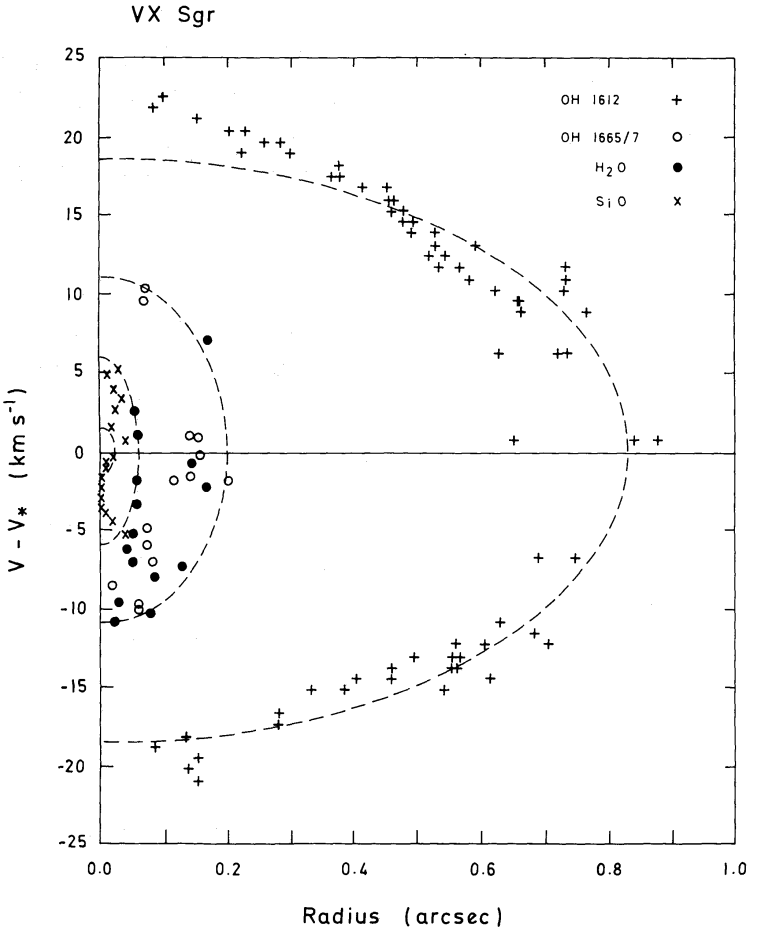

Figure 5. Radial velocities of the masers around VX Sgr relative to the stellar velocity are plotted against their angular separation from the assumed stellar position. Each dashed ellipse traces the expected position–velocity locus for a uniformly expanding spherical shell, as discussed in the text (Section 4.1).

represented in Fig. 5 by the outer dashed ellipse, and provides a good fit to the data. The expansion velocity of 19 km s^{-1} is obtained from the intersections of the ellipse with the y axis of zero spatial off-set, and the shell radius is given by the intercept with the x axis of zero expansion velocity.

The other masers in the inner region of the envelope have smaller spatial extent and smaller velocity range than the OH 1612-MHz masers. Their distribution is consistent with a regular velocity field in which the expansion velocity increases with distance from the star. The inner masers are located within well-defined elliptical boundaries in the position–velocity plot (Fig. 5). For the adopted alignments, the OH mainline and H_2O masers occur in a 'thick shell' region with inner radius $\sim 1.5\times10^{15}$ cm and outer radius $\sim 5\times10^{15}$ cm. The expansion velocity increases from $\sim$6 to $\sim$11 km s^{-1} across this region. It is interesting that the OH mainline and H_2O masers share the same kinematics, although their spatial distributions and excitation requirements are different (Section 4.3). These masers also tend to lie on the near side of the thick shell ($V-V_* < 0$). Their inner boundary is close to the outer boundary of the SiO masing region. The distribution and velocities of the SiO masers are consistent with their location in an expanding thick-shell region of mean radius $\sim 8\times10^{14}$ cm, as already pointed out by Lane (1984). A small zone of avoidance near the origin in Fig. 5 suggests that the SiO masers occur only at radii in excess of 5×10^{14} cm and with expansion velocities of 2 km s^{-1} or more.

We now examine the envelope kinematics in more detail.

4.2 VELOCITY STRUCTURE OF THE ENVELOPE

The elliptical boundaries of the maser regions shown in Fig. 5 give the expansion velocity of the circumstellar envelope at four radial distances. The data, plotted in Fig. 6, provide the first direct estimate of the velocity gradient at different radii in a circumstellar envelope. The important parameter governing maser amplification is the logarithmic velocity gradient

$$\varepsilon = \frac{d \ln V}{d \ln R} = \frac{R}{V}\frac{dV}{dR}.$$

We find $\varepsilon \sim 1.0$ in the region of the SiO masers, $\varepsilon \sim 0.5$ in the region of the H_2O and OH mainline masers, and $\varepsilon \sim 0.2$ in the region of the OH 1612-MHz masers. These values are higher than has

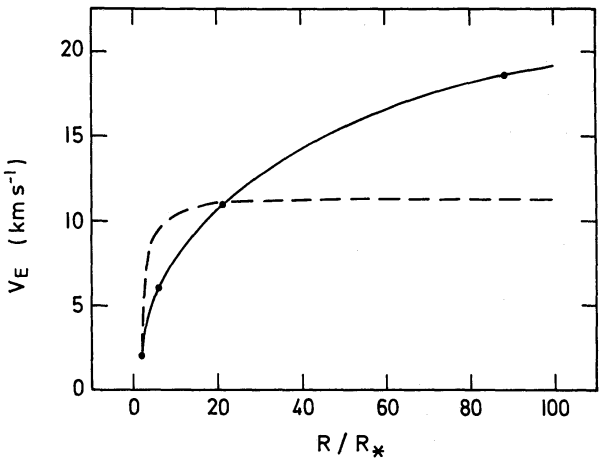

Figure 6. The expansion velocity of the circumstellar envelope plotted against the radial distance from the centre of the star in units of the stellar radius. The outer point was determined using the expanding envelope model by Reid *et al.* (1977) whilst the three inner points show the boundaries of the SiO, H_2O and OH mainline maser regions. The solid and dashed lines show theoretical velocity curves as discussed in the text (Section 4.2).

been assumed hitherto in theoretical modelling of the maser regions. In particular the OH 1612-MHz and mainline masers have generally been considered to arise in regions where $\varepsilon \sim 0.0$ (Goldreich & Scoville 1976; Elitzur 1978). A high value of $\varepsilon > 1$ was also inferred from observations of OH mainline masers in the source U Orionis (Chapman & Cohen 1985), although the argument in that case was indirect. It is important to establish observationally if such high values of ε are the rule or the exception. High values of ε would imply a higher pumping efficiency or a higher molecular density than has been considered so far.

To understand the possible causes of the high velocity gradients at large radial distances, we need to consider the envelope dynamics. The mass outflow from the circumstellar envelope of a late-type star is thought to be driven by radiation pressure acting on the circumstellar grains (e.g. Kwok 1975; Goldreich & Scoville 1976). If the only significant forces determining the envelope dynamics are from radiation pressure and gravity, then the equation of motion describing the gas flow is given by

$$V_{\mathrm{E}} \frac{dV_{\mathrm{E}}}{dR} = -\frac{GM_*}{R^2} + \frac{L_* \varkappa}{4\pi R^2 c}, \tag{2}$$

where V_{E} is the expansion velocity at the radius R, M_* is the stellar mass, L_* is the stellar luminosity and $\varkappa$ is the dust opacity per unit mass with

$$\varkappa = \frac{\sigma_{\mathrm{gr}} n_{\mathrm{gr}} Q}{\varrho}. \tag{3}$$

σ_{gr} and n_{gr} are respectively the cross-section and number density of the grains, ϱ is the gas density and Q is a radiation-pressure efficiency factor which is constant for optically thin envelopes. It is usually assumed that circumstellar grains condense at a few stellar radii so that for optically thin envelopes $\varkappa$ is constant beyond the grain condensation radius.

In Fig. 6 we plot V_{E} against R/R_* for the four data points and we show velocity curves obtained by integrating equation (2) with the stellar parameters $L_* = 4 \times 10^5\, L_\odot$, $R_* = 2.4 \times 10^{14}$ cm and $M_* = 10\, M_\odot$. The dashed line shows a model where $\varkappa = 0.4\,\mathrm{g\,cm^{-2}}$ is a constant chosen to fit the curve through the points at $R/R_* = 2$ and $R/R_* = 21$. This model clearly does not describe the velocity field of VX Sgr. The observed velocity curve increases less steeply and over a greater radial distance than predicted by a simple $1/R^2$ radiation pressure law. The data can, however, be described by a model in which $\varkappa$ is allowed to increase with R so that the radiation pressure becomes increasingly effective with distance from the star. This situation was considered by Goldreich & Scoville (1976) and following their model we adopt a function for $\varkappa$ given by

$$\varkappa = \Gamma \left(1 + \frac{AR^2}{B^2 R_{\mathrm{i}}^2 + R^2} \right), \tag{4}$$

where Γ, A and B are constants and R_{i} is the inner grain condensation radius. The solid curve shown in Fig. 6 is a fit to the data using this model. The inner boundary is taken to be at $R_{\mathrm{i}} = 2\, R_*$ where $V_{\mathrm{E}} = 2\,\mathrm{km\,s^{-1}}$. The parameters Γ, A and B for this model are $\Gamma = 0.32\, M_{10}\,\mathrm{cm^2\,g^{-1}}$, $A = 39\, M_{10}^{-1}$ and $B = 31$, where $M_{10} = M_*/10\, M_\odot$. The velocity curve is still rising at the radius of the OH 1612-MHz masers and reaches a terminal velocity of $24\,\mathrm{km\,s^{-1}}$. The opacity term $\varkappa$ increases monotonically with R from $\varkappa = 0.32\, M_{10}\,\mathrm{cm^2\,g^{-1}}$ at $R = 2\, R_*$ to a maximum value of $\varkappa_{\max} \simeq 13\,\mathrm{cm^2\,g^{-1}}$ (which is almost independent of M_*), and $\varkappa = 0.75\, \varkappa_{\max}$ at $R \simeq 105\, R_*$. For comparison, in the model by Goldreich & Scoville (1976), $\varkappa = 0.75\, \varkappa_{\max}$ at $R = 16\, R_*$.

The specific values obtained for the parameters Γ, A and B are clearly model dependent. Furthermore we have not considered the effect of departures from spherical symmetry in the flow. Nevertheless, we expect that a fully detailed model including all contributing factors will not

significantly alter the conclusion that in the circumstellar envelope the opacity per unit mass increases to a radial distance of at least $50\,R_*$ or $\sim 1.3\times10^{16}$ cm, considerably greater than has been previously considered. One possible explanation is that, as the temperature drops, icy mantles grow on the surfaces of silicate grains, increasing the grain cross-sections and hence increasing $\varkappa$ (Jura & Morris 1985). Observational evidence on the variation of $\varkappa$ with R is sparse. Lunar occultation measurements of the Mira variable IRC 10011 suggest that dust emission occurs to at least $15\,R_*$ (Zappala *et al.* 1974). Infrared speckle and interferometric techniques may be expected to contribute important new data on this problem in the near future.

4.3 ENVELOPE ASYMMETRIES

The maps of the H_2O and OH mainline masers indicate an asymmetry in the inner regions of the circumstellar envelope of VX Sgr. Although the assumed stellar position maximizes the envelope symmetry and indeed leads to a spherically symmetric model for the velocity field, the actual distributions of the H_2O and OH mainline masers as projected on the sky are *not* symmetric. The H_2O masers show a distribution which is elongated east–west whilst the OH mainline masers are elongated approximately north–south. For the small numbers of observed masers, it is possible that these asymmetric distributions could have arisen by chance. They could also be time dependent, as the H_2O and OH mainline masers are variable. However, a fundamental asymmetry is indicated by the fact that the H_2O and OH mainline masers require different physical conditions for their excitations. In particular, H_2O masers are thought to require higher gas densities and temperatures.

Theoretical models predict that for a high mass-loss star such as VX Sgr, the H_2O emission should occur at $\sim10^{15}$ cm (Cooke & Elitzur 1985). At this radius most of the oxygen is thought to be contained in H_2O rather than in OH. Greater column densities of OH are expected further out in the envelope, where OH is produced by photo-dissociation of H_2O in the external ultraviolet (UV) radiation field (Goldreich & Scoville 1976; Scalo & Slavsky 1980). The radius at which this occurs depends on the distance to which the UV photons can penetrate the circumstellar envelope, and is greater for envelopes with higher mass-loss rates (Huggins & Glassgold 1982).

We have considered three ways in which the differences between the theoretical models and our observations might be resolved:

(i) One possibility is that the adopted alignment of the OH mainline masers with the H_2O masers (Section 4.1) is incorrect and that the OH mainline masers are in fact located at larger radii than the H_2O masers. This would indicate an extreme asymmetry in the distribution of the OH mainline emission, as is seen in OH 127.8–0.0 (Diamond, Norris & Booth 1985). Since the OH mainline emission from VX Sgr covers a wide range of velocities, it seems implausible that such a turbulent cell would form at a large radius ($\sim10^{16}$ cm) where the velocity field otherwise shows little turbulence. We therefore regard this possibility as very unlikely.

(ii) A second possibility is that the mass loss is extremely asymmetric and that this asymmetry allows the external UV radiation to penetrate the envelope and photo-dissociate H_2O at radii of $\sim10^{15}$ cm. This could occur if the circumstellar envelope of VX Sgr had a bipolar structure. In this model the H_2O and OH 1612-MHz masers are located in an east–west doughnut where the gas density is greatest for a given radius, and the OH main-line masers are located north–south where the gas density is least. In the east–west direction the peak density of OH molecules would occur at a radial distance of about 2×10^{16} cm where the gas temperature is sufficiently low to favour the 1612-MHz transition. In this plane the H_2O molecules are closer to the star than the OH molecules. In the north–south direction, the H_2O molecules would photo-dissociate to OH molecules at a smaller radius of approximately 3×10^{15} cm where the temperature is higher, and the OH maser lines at 1665/7 MHz are excited.

(iii) A third possibility is that the asymmetry in the mass loss is less extreme but sufficient to allow OH mainline emission to be excited at radii of $\sim 10^{15}$ cm by a fairly efficient pumping scheme. Calculations by Elitzur (1978) indicate that the OH mainline pumping efficiency rises with temperature since higher rotational levels excited at temperatures of ~300 K also contribute significantly to the ground-state population inversion. This possibility needs further investigation.

Of these three possibilities we favour the second and third. Whichever is correct, it is clear that the mass loss is asymmetric, and the mass-loss rate would therefore be overestimated in any model which assumed spherical symmetry.

4.4 THE STELLAR MAGNETIC FIELD

The OH mainline maser emission from VX Sgr is variable and strongly circularly polarized. The circular polarization results from Zeeman splitting of spectral lines in the stellar magnetic field (Cook 1966). A Zeeman pattern is suggested by the near coincidence in the measured positions and velocities of several features at 1665 and 1667 MHz (Fig. 3 and Tables 1 and 2). Single-dish

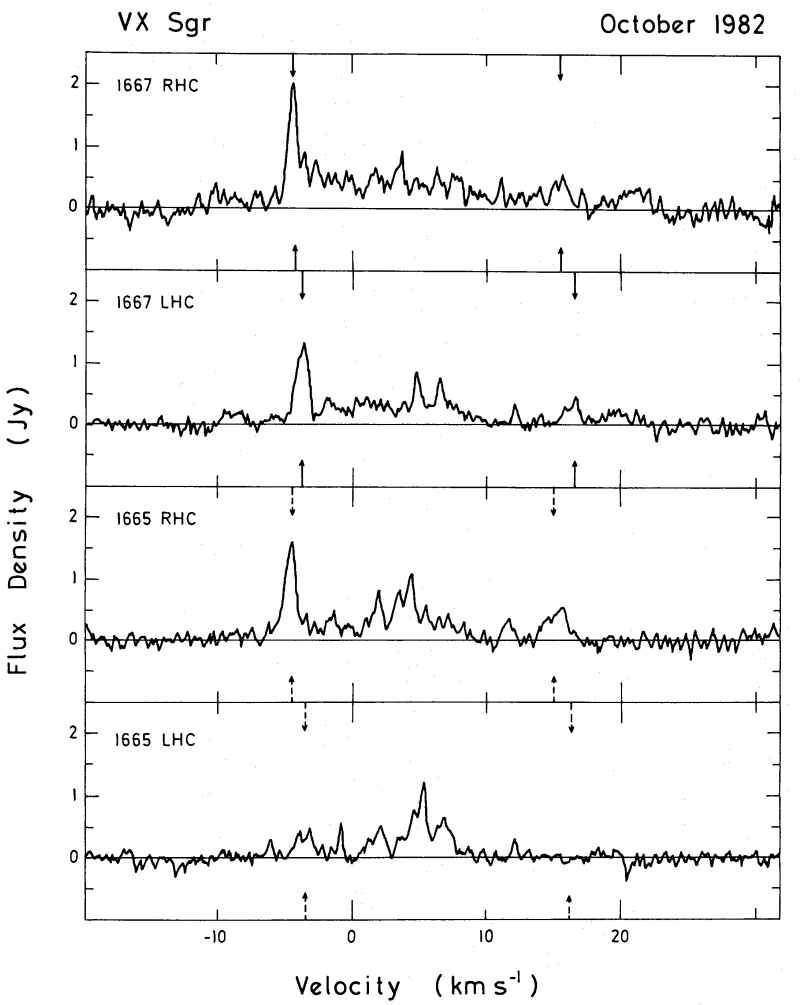

Figure 7. Mainline OH spectra of VX Sgr taken with the Jodrell Bank MKIA radio telescope in 1982 October. The velocity resolution is 0.19 km s^{-1}. Two Zeeman groups at velocities near −4 and +16 km s^{-1} are indicated by vertical arrows. The solid arrows show the 1667-MHz velocities determined by Gaussian fitting, and the dashed lines show the corresponding velocities expected at 1665 MHz for pure Zeeman splitting (see Section 4.4 and Table 4).

spectra of the OH mainline emission are shown in Fig. 7. From the spectra and the positions of the OH mainline masers, two Zeeman groups can be clearly identified. The peak velocities of these lines determined by fitting Gaussian profiles through the single dish spectral features are listed in Table 4. For these two groups the 1665- and 1667-MHz RHC features are spatially coincident (Fig. 3). In Fig. 7 the 1667-MHz LHC–RHC pairs are indicated by solid arrows, and the velocities expected for the corresponding 1665-MHz LHC–RHC pairs are indicated by the dashed arrows. There is good agreement between the predicted and measured velocities of the 1665-MHz features. For the group of features near $-4\,\mathrm{km\,s^{-1}}$ a complete Zeeman quartet is seen corresponding to a magnetic field of -1.8 ± 0.4 mG. For the group of features near $16\,\mathrm{km\,s^{-1}}$, only three features of the Zeeman pattern are present and the implied magnetic field is -2.5 ± 0.4 mG. The field is directed towards us in both cases. The distances of these masers from the centre of the star is $\sim3\times10^{15}$ cm in our model of the circumstellar envelope (Sections 4. 1 and 4.2). Assuming a solar type $1/R^2$ radial dependence of the magnetic field (Parker 1963), the field at the stellar photosphere is approximately 0.5 G. This is comparable to the quiescent field strength of the solar photosphere.

The magnetic field of ~2 mG at a radius of 3×10^{15} cm has an energy density comparable to the kinetic energy density of the outflowing gas, and so the magnetic field may be expected to influence the envelope dynamics. The charged dust grains will be coupled to the stellar magnetic field and they in turn drive the outflow through collisions with the gas. This could provide a possible explanation for the asymmetric mass loss.

There is also indirect evidence for a significant magnetic field at the larger distance of the OH 1612-MHz masers. High-resolution spectra of the 1612-MHz emission reveal narrow polarized components (Cohen 1985). These indicate magnetic fields of order mG at radii of 2×10^{16} cm, which could be produced by magnetic 'hotspots' of ~10 G at the stellar photosphere.

If the magnetic fields of stars such as VX Sgr change periodically then the variation in field intensity may be reflected in the observed distribution of the masers and in the Zeeman splitting of the spectral lines. Repeated aperture synthesis and single-dish observations of highly polarized stellar masers, possibly using all four Stokes parameters, could provide valuable insight into the magnetic field behaviour of these high mass-loss stars.

Table 4. Velocities of features identified with Zeeman Groups – 1982 October.

Freq MHz	Poln	Feature A Velocity (km s^{-1})	Feature B Velocity (km s^{-1})
1665	LHC	-3.5 ± 0.4	- (weak)
1665	RHC	-4.6 ± 0.1	15.3 ± 0.1
1667	LHC	-3.7 ± 0.1	16.5 ± 0.1
1667	RHC	-4.3 ± 0.1	15.6 ± 0.1

5 Conclusions

VX Sgr is the first star for which there are interferometer maps of all the radio maser lines: VLBI observations of SiO masers by Lane (1984) and the present MERLIN observations of H_2O and OH masers. The masers form a natural sequence in which the velocity extent of the emission increases systematically with angular extent. This result is independent of the assumed stellar position, and suggests a regular velocity field in which expansion velocity increases outwards with radial distance in the circumstellar envelope. By assuming that the emission centroids of the

different maser lines coincide with the stellar position, it has been possible to construct a detailed picture of the circumstellar envelope. With the adopted stellar position it is found that the high-excitation SiO masers trace the innermost region of the envelope, the H_2O and OH mainline masers trace a thick layer surrounding this, and on the OH 1612-MHz masers trace a cool outer shell. The velocity gradient through the region of H_2O and OH mainline masers is greater than has been considered hitherto in theoretical models of these maser regions (Section 4.1). This can be understood in terms of an increase in the driving force per unit mass with distance from the star, which could in turn be produced by condensation of grain material out to distances of at least 50 stellar radii. It is important to confirm this result by measuring the absolute positions of the H_2O and OH mainline masers.

The spatial structure of the envelope shows considerable asymmetries which are particularly evident in the inner regions. This suggests an intrinsic asymmetry in the mass-loss process. One possible cause for this is the stellar magnetic field. Zeeman splitting of the OH mainlines indicates a field of ~ 2 mG at radii of $\sim 3 \times 10^{15}$ cm. This field is strong enough to channel the outflow, the gas flow being coupled to the magnetic field by charged dust grains. This could explain in a natural way the bipolar structure which is suggested by our results. The influence of stellar magnetic fields on mass loss in late-type stars has not been included in theoretical models, and a detailed consideration of these effects is necessary.

Acknowledgments

We thank Angela Bayley, Drs P. Thomasson and B. Anderson and Professor J. G. Davies for their assistance with the MERLIN observations and Professor R. Booth for his comments on the manuscript.

References

Booth, R. S., Kus, A. J., Norris, R. P. & Porter, N. D., 1981. *Nature,* **291,** 382.
Bowers, P. F., Johnston, K. J. & Spencer, J. H., 1981. *Nature,* **291,** 382.
Chapman, J. M. & Cohen, R. J., 1985. *Mon. Not. R. astr. Soc.,* **212,** 375.
Cohen, R. J., 1985. *Cosmic Gas Dynamics,* in press, ed. Kahn, F. D., Manchester University Press.
Cook, A. H., 1966. *Nature,* **211,** 503.
Cooke, B. & Elitzur, M., 1985. *Astrophys. J.,* **295,** 175.
Cornwell, T. J. & Wilkinson, P. N., 1981. *Mon. Not. R. astr. Soc.,* **196,** 1067.
Diamond, P. J., Norris, R. P. & Booth, R. S., 1985. *Mon. Not. R. astr. Soc.,* **216,** 1P.
Diamond, P. J., Norris, R. P., Rowland, P. R., Booth, R. S. & Nyman, L.-A., 1985. *Mon. Not. R. astr. Soc.,* **212,** 1.
Elitzur, M., 1978. *Astr. Astrophys.,* **62,** 305.
Elitzur, M., 1980. *Astrophys. J.,* **240,** 553.
Elitzur, M., 1981. *Physical Processes in Red Giants,* p. 363, eds Iben, I. & Renzini, A., Reidel, Dordrecht, Holland.
Elitzur, M., 1982. *Rev, Mod. Phys.,* **54,** 1225.
Elitzur, M., Goldreich, P. & Scoville, N., 1976. *Astrophys. J.,* **20,** 47.
Engels, D., Kreysa, E., Schultz, G. V. & Sherwood, W. A., 1983. *Astr. Astrophys.,* **124,** 123.
Goldreich, P. & Scoville, N. Z., 1976. *Astrophys. J.,* **205,** 144.
Högbom, J. A., 1974. *Astr. Astrophys. Suppl.,* **15,** 417.
Huggins, G. & Glassgold, A. E., 1982. *Astr. J.,* **87,** 1828.
Humphreys, R. W., 1974. *Astrophys. J.,* **188,** 75.
Humphreys, R. W., Strecker, D. W. & Ney, E. P., 1972. *Astrophys. J.,* **172,** 75.
Johnston, K. J., Spencer, J. H. & Bowers, P. F., 1985. *Astrophys. J.,* **290,** 660.
Jura, M. & Morris, M., 1985. *Astrophys. J.,* **292,** 487.
Kukarkin, B. V., Kholopov, P. N., Efremov, Yu. N., Kukarkina, N. P., Kurochkin, N. E., Medvedeva, G. I., Perova, N. B., Federovich, V. P. & Frolov, M. S., 1970. *Catalogue of Variable Stars,* Astronomical Council of the Academy of Sciences in the USSR, Moscow.
Kwok, S., 1975. *Astrophys. J.,* **198,** 583.

Lane, A. P., 1984. *IAU Symp. No. 110,* p. 329, eds Fabnti, R., Kellermann, K. & Setti, G., Reidel, Dordrecht, Holland.
Olnon, F. M., 1977. *PhD thesis,* University of Leiden.
Paczyński, B., 1970. *Acta Astronomica,* **20,** 47.
Parker, E. N., 1963. *Interplanetary Dynamical Processes,* John Wiley & Sons, New York.
Reid, M. J., Muhleman, D. O., Moran, J. M., Johnston, K. J. & Schwartz, P. R., 1977. *Astrophys. J.,* **214,** 60.
Scalo, J. M. & Slavsky, D. B., 1980. *Astrophys. J.,* **239,** L73.
Zappala, R. R., Becklin, E. E., Mathews, K. & Neugebauer, G., 1974. *Astrophys. J.,* **192,** 109.